Chemical Engineering Journal 406 (2021) 126749

Contents lists available at ScienceDirect

Chemical Engineering Journal

journal homepage: www.elsevier.com/locate/cej

Synergetic effects of metals in graphyne 2D carbon structure for high promotion of CO_2 capturing

Mohammad Hossein Darvishnejad[a], Adel Reisi-Vanani[a,b,*]

[a] Department of Physical Chemistry, Faculty of Chemistry, University of Kashan, Kashan, Iran
[b] Institute of Nano Science and Nano Technology, University of Kashan, Kashan, Iran

HIGHLIGHTS

- CO_2 capture behavior of co-decorated GY by Sc and Cr atoms was investigated.
- In SCGY, synergetic effect of Cr and Sc atoms causes that E_{ads} improves ~0.505 eV.
- Increasing of E_{ads} due to insertion of one or two metal atoms is ~3 to 12 times more than PGY.
- The best system can capture up to 19 CO_2 molecules with $\bar{E}_{ads}$ of −0.516 eV/CO_2.
- CO_2 storage capacity of the best system is 55.66 wt%.

ARTICLE INFO

Keywords:
2D carbon structure
Graphyne
Metal co-decorated
CO_2 capture
DFT-D3
Adsorption

ABSTRACT

Structural and electronic properties of co-decorated graphyne (GY) by Sc and Cr atoms toward CO_2 capture are investigated by DFT-D3 method. First, different configurations of Sc-Cr co-decorated GY (SCGY) are considered to find the best site and side of GY for SC and Cr atoms and structural, magnetic, and electronic properties of them are investigated. Then, the adsorption behavior of the best configurations toward CO_2 capture is followed. Results show that in single Sc or Cr decorated GY, the best site for metals is the center of the 12-membered ring (H1) and E_{ads} are −4.856 and −2.414 eV, respectively. In SCGY, the best site for Cr and Sc are H1 and H3 sites, but they lie in the opposite sides and E_{ads} improves about 0.505 eV. In brief, E_{das} of CO_2 for pristine GY (PGY), Sc-GY, Cr-GY, Sc-Cr-GY, Sc-Sc-GY, and Cr-Cr-GY are about −0.242, −0.717, −1.502, −0.795, −2.970 and −1.754 eV, respectively. Increasing of E_{ads} due to the insertion of one or two metal atoms for some systems is about 3 to 12 times more than PGY, surprisingly. The best system can capture up to 19 CO_2 molecules with of −0.516 eV/CO_2 that is CO_2 storage capacity of 55.66 wt%. These results show that co-decorated GYs with various metals, due to having synergistic effects, can be used as promising candidates for the CO_2 capture, storage, detection, and removal applications in the future.

1. Introduction

In recent years due to the great consumption of fossil fuels and industrial activities, production of carbon dioxide in the atmosphere is rising dramatically. CO_2, the most important greenhouse gas, is the main cause of global warming [1,2]. So, one of the major challenges to protect the environment is the capture, storage, and conversion of CO_2 [3–5]. Recently, one of the novel approaches to CO_2 capture and storage is the use of developed solid materials such as two-dimensional (2D) nanomaterials. For example, hexagonal boron nitride [6,7], carbon nitride [8,9], aluminum nitride [10], graphene [11,12], borophene and phosphorene [13,14] nanostructures have been widely considered by researchers for CO_2 capture and storage. Among these 2D nanostructures, graphene families due to the large surface area, high adsorption capacity, tunable electronic properties, uniformly distributed pores and capable of surface modification is a promising candidate for CO_2 capturing [15,16].

A new member of the graphene family, which was suggested by Baughman et al. in 1987, is graphyne (GY) [17]. It has the same symmetry as grapheme but its carbon hybridization type is different from graphene. GY consists of sp and sp^2 carbon atoms, also in its lattice structure, benzene rings connected by acetylenic bonds (–C≡C–) [17–19]. With different ratio of –C≡C– bonds, various structures of GY are formed, such as α-, β-, γ-, 6,6,12-, 14,14,14, 14,14,18 and so on

* Corresponding author at: Department of Physical Chemistry, Faculty of Chemistry, University of Kashan, Kashan, Iran.
E-mail address: areisi@kashanu.ac.ir (A. Reisi-Vanani).

https://doi.org/10.1016/j.cej.2020.126749
Received 5 May 2020; Received in revised form 20 July 2020; Accepted 19 August 2020
Available online 27 August 2020
1385-8947/

[18,20–22]. Among all types of GYs, γ-GY has some benefits such as higher stability and semiconductor property, and is used and studied more than other types [23]. Newly studies have shown that the GY family has physical, chemical and electrical performance more than graphene, and these systems can be frequently proposed for some technological applications such as optics [24–27], transistors [28], hydrogen storage [29–31], electrode in batteries [32,33], separation/purification membranes for gas purification [34], gas sensor [35,36] and catalysis [37–39].

Recent researches show that GY can be a promising candidate for the storage, capture, and conversion of gases [40–45]. One of the effective ways to increase gas capture and storage is the surface modification or surface functionalization; because, dispersion and specific interactions affected by chemical functional groups of the carbon frame can better adsorb small gas molecules [46]. For this purpose, researchers modify the surface by non-metal doping or metal decoration. GY based materials properties such as structural, electronic, optical, magnetic, and other properties can be tuned by doping with non-metal and decoration with transition metal atoms [47–49]. For example, interaction between GY and some of the 3*d* transition metals (Sc to Cu) was investigated using DFT by Ren *et al.* The results demonstrate that electronic and magnetic properties of GY are tuned by TM atoms. These results show that TM decorated GY nanostructures are profitable for magnetic and spintronic applications, potentially [50]. Mofidi and Reisi-Vanani investigated the interaction between Li, Ti, Fe and Ni-decorated GY with Sarin toxic gas [42]. The results showed that these compounds have great potential for sensing and capturing sarin. Adsorption of several gas molecules such as O_2, CO_2, CO, NH_3, CH_4 and NO on the PGY and Mn-decorated GY was considered by Lu *et al.*, computationally [51]. Their results specify that there are chemical interactions between Mn-decorated GY and all of these small molecules except O_2. So, it can be said that the adsorption of these molecules significantly improves by adding Mn atoms to GY sheet. Zhang and Wu employed DFT calculations to evaluate the Ni, Cr and Pd-decorated GY as versatile materials for energy storage. The analysis of the electronic properties of these structures demonstrates that they are promising structures for energy storage [49]. The interaction between Sc and Ti-decorated graphdiyne with formaldehyde was considered by Chen *et al.*, theoretically [52]. The results exhibit that these materials have a good electronic response and can be used as high efficient detectors of formaldehyde.

In this work, we investigate structural, magnetic and electronic properties of co-decoration of GY by two metals (Sc and Cr) for the first time, systematically to specify: (i) the synergetic effect of Sc and Cr atoms on the structural, electronic and magnetic properties of GY; (ii) adsorption behavior of single CO_2 onto various SCGY systems; (iii) the maximum number of CO_2 captured on the SCGY sheet. The results show that Sc and Cr atoms have a synergetic effect to promote capture and storage of CO_2 onto GY, dramatically and these systems can be suggested as suitable candidates for CCS technology.

2. Computational details

All calculations related to geometry optimization, adsorption of transition metals, capture of CO_2, electronic properties, and charge distribution were carried out by spin-polarized DFT method using $DMol^3$ module [53] implemented in Materials Studio software. All calculations were done with the generalized gradient approximation (GGA) method with Perdew-Burke-Ernzerhof (PBE) [54] as exchange–correlation functional, as well the double numerical plus polarization (DNP) basis set [55]. The DFT semi core pseudo-potential (DSPP) was applied for the relativistic effect to treat the core electrons, which replaces a single effective potential instead of the core electrons. For dispersive intermolecular interactions and long-range Van der Walls forces, DFT-D3 method proposed by Grimme was used in all calculations [56–58]. In all calculations, we used a 2 × 2 supercell for sample of GY in which a vacuum space of 20 Å in *z* direction applied in order to avoid the interlayer interactions. To integrate the Brillouin zone, we used a 7 × 7 × 1 gamma centered Monkhorst-Pack mesh of k-grid sampling. Without imposing any symmetry limitations, all atoms were allowed to relax. The values of 10^{-5} Ha, 2×10^{-3} Ha Å^{-1}, 5×10^{-3} Å and 5.0 Å were chosen as energy tolerance accuracy, maximum force, displacement and global orbital cut-off radius, respectively. Estimation of adsorption energy (E_{ads}), when transition metal atoms adsorbed on the GY sheet, was done using the following equation:

$$E_{ads} = E_{GY-TMs} - (E_{GY} + E_{TMs}) \quad (1)$$

in which E_{TMs}, $E_{GY,}$ and $E_{GY\text{-}TMs}$ are the total energy of TM atoms, intact GY and TM decorated or co-decorated GY, respectively. For estimation of the adsorption energy of CO_2 onto decorated GY, we used two following equations, first for the average binding energy ($\bar{E}_{ads}$) and the second for the energy of each step (E_s):

$$\bar{E}_{ads} = [E_{TMs-GY-nCO2} - (E_{TMs-GY} + nE_{CO2})]/n \quad (2)$$

$$E_s = E_{TMs-GY-nCO2} - (E_{TMs-GY-(n-1)CO2} + E_{CO2}) \quad (3)$$

where $E_{TMs\text{-}GY\text{-}nCO2}$, $E_{TMs\text{-}GY\text{-}(n\text{-}1)CO2}$, $E_{TMs\text{-}GY,}$ and E_{CO2} are the total energy of the complex of TMs decorated or co-decorated GY and nCO_2, TMs decorated or co-decorated GY and (n-1) CO_2, TMs decorated and co-decorated GY and isolated CO_2 molecule, respectively. Also, the number of adsorbed CO_2 molecules has been shown with *n* in these equations. To better understand the adsorption behavior of Sc and Cr atoms or CO_2 molecule onto PGY and decorated or co-decorated GY, Hirshfeld charge analysis was done in all calculations.

3. Results and discussion

3.1. Structural and electronic properties of the PGY and single Sc or Cr-decorated GY and evaluation of CO_2 adsorption on them

In our previous work, we studied single atom decoration of GY by all of the 3*d* and 4*d* series of transition metals, and the adsorption behavior of those systems has been brought and discussed in details [59]. Then, the adsorption behavior of CO_2 onto all of them was investigated. Results showed that for single Sc or Cr atom decoration of GY, during the optimization process and for all of seven examined sites, TM atom only would gradually move to H2 (center of hexagonal) or H1 sites. The optimized structures and the calculated structural properties of Sc and Cr-decorated GY in H1 and H2 sites have been brought in Fig. 1 and Table 1.

According to Table 1, the H1 site is more desirable than the H2 site for Sc and Cr decoration, energetically and high values of E_{ads} show that their adsorption mechanisms are chemisorption. These results are in good agreement with the previous theoretical study [47,50,60,61]. Also, the results show that PGY is a semiconductor with a spin-degenerated direct-band-gap of 0.432 eV, in which a maximum of the valence band and minimum of conduction band are exactly at the gamma point. It is consistent with other works [41,62]. As well, the spin-up and spin-down band structure of the Sc-decorated GY are the same with a band gap of zero, so this system has no magnetic moment. It shows semi-metallic properties because of crossing its conduction band with the Fermi level. Our findings also show that the adsorption of Cr atom on GY induces spin splitting of the band structures with a band gap of zero and produces the magnetic moment for Cr-decorated GY. Also, the Cr-decorated GY structure shows semi-metallic properties, which is in agreement with other works [50,60]. Charge values of the Sc and Cr atoms, when GY is decorated with them in the H1 site, are about 0.584 and 0.431 *e*, respectively. Because, Sc and Cr atoms give part of their 4*s* electrons to the empty π* states of the GY.

Fig. 2 shows the spin-polarized partial density of state (PDOS) diagrams of the intact GY, Sc, and Cr-decorated GY (in H1 site). In these images, contributions of C_{sp} and C_{sp2}, as well Sc and Cr metals, besides

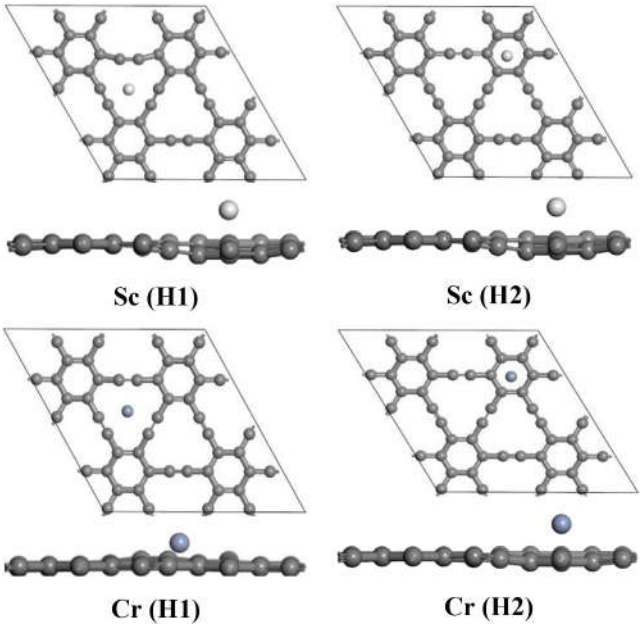

Fig. 1. Optimized structures of single Sc and Cr atoms decorated GY in H1 and H2 sites from top and side views.

Table 1
The most favorable sites, the distance between Sc or Cr atoms and GY sheet (d in Å), adsorption energy (E_{ads}), band gap (E_g), Fermi energy level (E_f) (in eV) and Hirshfeld charge transfer of Sc and Cr atoms in various sites (*e*).

Structures	Site	d	E_{ads}	E_g	Charge of TM
PGY	–	–	–	0.432	–
Sc-decorated GY	H1	1.252	−4.856	0.000	0.584
Sc-decorated GY	H2	1.724	−3.965	0.000	0.271
Cr-decorated GY	H1	0.663	−2.414	0.000	0.431
Cr-decorated GY	H2	1.462	−0.456	0.372	0.127

the total system have been figured, separately. The analysis of PDOS gives insight information about the binding mechanism and interaction between Sc and Cr atoms with PGY. In all of the PDOS plots, the Fermi level was set to zero. It is seen that for PGY, a major contribution in the states close to the Fermi level is related to the 2*p* orbitals of C_{sp2} and C_{sp} atoms (Fig. 2 (a)), and 2*s* orbitals have no contribution in this region. As shown in Fig. 2 (b) and (c), there is no symmetry between DOS image related to spin-up and spin-down states for C_{sp2}, $C_{sp,}$ and Cr atoms in Cr-decorated GY, while spin-up and spin-down diagrams of Sc-decorated GY are the same, and no spin polarization observes. So, unlike Sc-decorated GY, Cr-decorated GY has magnetic property. Also, Sc and Cr atoms have relative low ionization potentials, so they easily donate some of their 4*s* electrons to the carbon frame. A part of this donated electrons transfers to the empty π* bands of the GY sheet and other part back-donates to 3*d* orbitals of the Sc and Cr atoms [49]. The interaction between Sc or Cr atoms with the GY sheet was augmented by hybridization between C 2*p* orbitals and Sc and Cr 3*d* orbitals. PDOS diagrams also confirm that unlike PGY, for Sc and Cr decoration of GY, the crossing of conduction bands with the Fermi level confirms that these systems show semi-metallic character and conductivity with zero band gaps.

3.2. Evaluation of the structural and electronic properties of the Sc-Cr co-decorated GY (SCGY)

Recently, co-doped GYs family for improving their practical applications has been suggested by researchers [11,31,63,64]. Here, with respect to our previous work, that reveals Cr-decorated and Sc-decorated GY have the highest interaction energy with CO_2 among other 3*d* TMs decorated GY systems [59], we chose Sc and Cr atoms for consideration of co-decorated GY by them, perhaps their synergy causes great improvement in not only CO_2 adsorption but also other structural and electronic properties of GY [65–69]. First, to find the best sites for co-decoration and the most stable structures, we investigated some of the possible configurations, namely, we fixed Cr in the H1 site and changed Sc position in seven different sites around Cr atom. These sites contain H1, H2 (center of rings), B1, B2, B3 (top of three types of bonds), T1 and T2 (top of two types of carbons). Also, we selected three different configurations of GY for Sc and Cr atoms, namely up-up, up-down and down-up sides, therefore 21 different initial structures were created that called **S1**-**S21** in Fig. 3 and Table 2. Also, in the structures **S22**-**S25**, we put two Sc or two Cr atoms in two adjacent H1 sites (once in the same sides and the other in opposite sides). Then, designed configurations were optimized without any constraint. Optimized structures and some results have been presented in Fig. 3 and Table 2. However, some of the final and optimized structures are similar, such as **S2** and **S3** with the same results. But, some of them are almost alike with small differences and with almost near adsorption energies such as **S9**, **S11**, **S12**, **S14**, **S15**, **S17** and **S21**.

Investigation of the results in Table 2 shows that after geometry optimization, for the most of SCGY structures H1 and H3 sites (H3 is the position of Sc atom (white atom) in **S9** structure in Fig. 3 or corner of the 12-membered ring) are more favorable than other sites for Cr and SC atoms, respectively (**S9**, **S11**, **S12**, **S14**, **S15**, **S17** and **S21**). After that, the H1 site for two decorating metals is the best site (**S2** and **S3**). It seems that the large size of the acetylenic ring organized by the C_{sp2} and C_{sp} bonds and existence of the inhomogeneous π-bindings between various hybridized carbon atoms in GY causes that metal atoms can approach better to the GY plane and form stronger interactions with carbon atoms. Also, when two different metals lie on opposite sides, the configuration is more stable than they are on the same sides. Also, using from Sc and Cr atoms as decorating metals is better than using from two similar metals. Therefore, it can say that configurations with Sc and Cr atoms in H3 and H1 sites and opposite sides are the most stable configurations (**S2**, **S3**, **S9**, **S11**, **S12**, **S14**, **S15**, **S17** and **S21**). Comparison of E_{ads} of these nine configurations reveals that stability of the structures with two metal atoms in opposite sides of an acetylenic ring (H1 or H3) is almost equal to when two metal atoms are in opposite sides and two adjacent H1 hollow sites. Of course, the first is a little more stable than the latter. Generally, **S9** configuration with E_{ads} of the second metal (Sc) about −5.361 eV is the most configuration among all of them. With respect to this adsorption energy and E_{ads} of the first metal (Cr) that was about −2.414 eV, one can say that adsorption mechanisms of these metals on the GY sheet are chemisorption. In absence of Cr atom, E_{ads} of Sc on GY is −4.856 eV, so it is expected that when Sc and Cr atoms were adsorbed on GY, sum of the adsorption energy will be −7.270 eV, while it is about −7.775 eV in the most stable configuration (**S9**) (Tables 1 and 2). It seems that Sc and Cr have a synergetic effect about −0.505 eV (!) on this E_{ads}. Even, for **S22** to **S25** structures with two equal metal atoms, this synergetic effect is seen. This finding can be used when it is necessary to improve the adsorption energy of the metals on carbon frames in practical applications.

It seems that when the first metal atom binds to the carbon frame, charge transfer happened between them and metal atom gives some of the 4*s* electrons to the carbon frame, then back donation of some of these electrons to empty 3*d* orbitals of metals is done. Besides, hybridization of 3*d* orbitals of metal atoms with π/π* states of carbon atoms takes place (Tables 1 and 2). So, E_{ads} of the metal atom to GY sheet is partly high. When the second metal atom approaches to metal decorated GY, the carbon frame is electron-rich. Therefore, it can better bind to second metal atoms and further charge transfer happens between them. There is a difference between SCGY systems from the viewpoint of E_{ads} when two metal decorating atoms are the same (**S22**

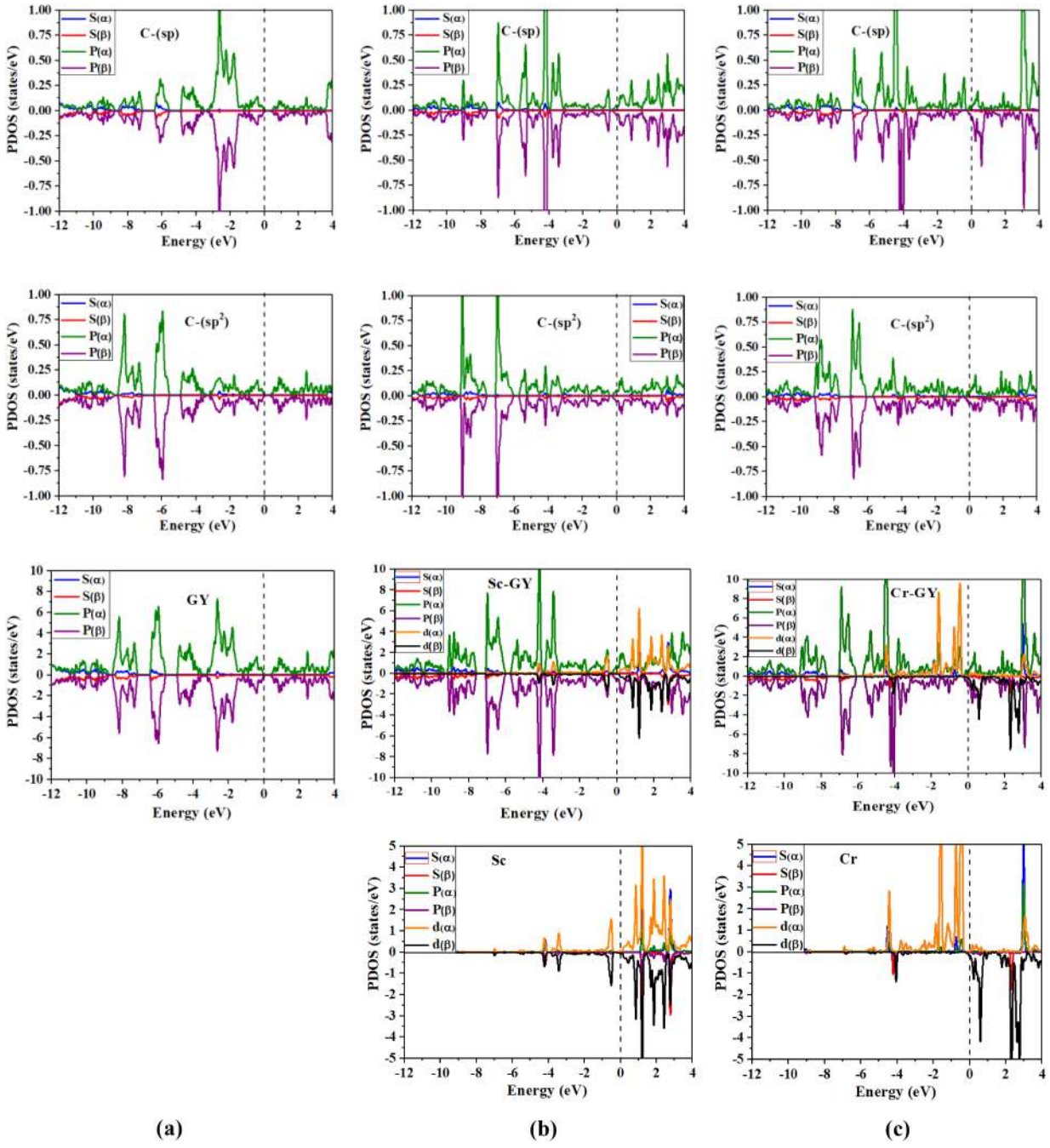

Fig. 2. PDOS images of: (a) intact, (b) Sc-decorated, and (c) Cr-decorated GY systems.

to **S25**) or different (**S1** to **S21**). It is seen that for the first systems with similar decorating metal atoms, up-up configurations are more stable than up-down ones, while for the latter with different decorating metal atoms, up-down configurations are more stable (Table 2).

Fig. 4 demonstrates spin-polarized electronic band structure diagrams for more stable structure of SCGY. However, PGY is a semiconductor with a direct band gap of 0.432 eV, but the insertion of metal atom causes that its electronic band structure changes and its conduction bands cross the Fermi level and all of these systems find semimetallic character due to this metal insertion [50]. As shown in Fig. 4, unlike **S9** and **S22**, which spin-up and spin-down states are the same and no spin polarization is observed, for **S24** system, a spin-polarized electronic band structure obtained. So, it can say **S9** and **S22** structures have no magnetic moment but **S24** shows magnetic character. Also, the **S24** structure shows semi-metallic properties, which is in good agreement with an earlier theoretical work [50].

Fig. 5 shows the spin-polarized PDOS diagrams of the **S9**, **S22** and **S24** structures that were segmented to C_{sp}, C_{sp2}, Sc and Cr atoms, as well total of these systems. Higher adsorption energy and type of decorating metals of the structures (Table 2) are reasons for selection of these structures (**S9**, **S22** and **S24**) for further investigation. As shown in Fig. 5, in **S9, S22** and **S24** structures, the states near the Fermi level are mostly composed of 3*d* orbitals of Sc and Cr atoms and 2*p* orbitals of the C_{sp} and C_{sp2} atoms. Also, *s* orbitals have no significant contribution to the states near the Fermi level. As well, the Sc and Cr 4*s* orbitals participate in non-bonding states higher than the Fermi level. This topic confirms Sc and Cr atoms donate part of their 4*s* electrons to the empty π^* bands of the GY. Furthermore, significant overlaps between π/π^* states of the carbon atoms and 3*d* and 4*s* orbitals of the Sc and Cr atoms indicate that there are strong interactions between metal atoms and GY

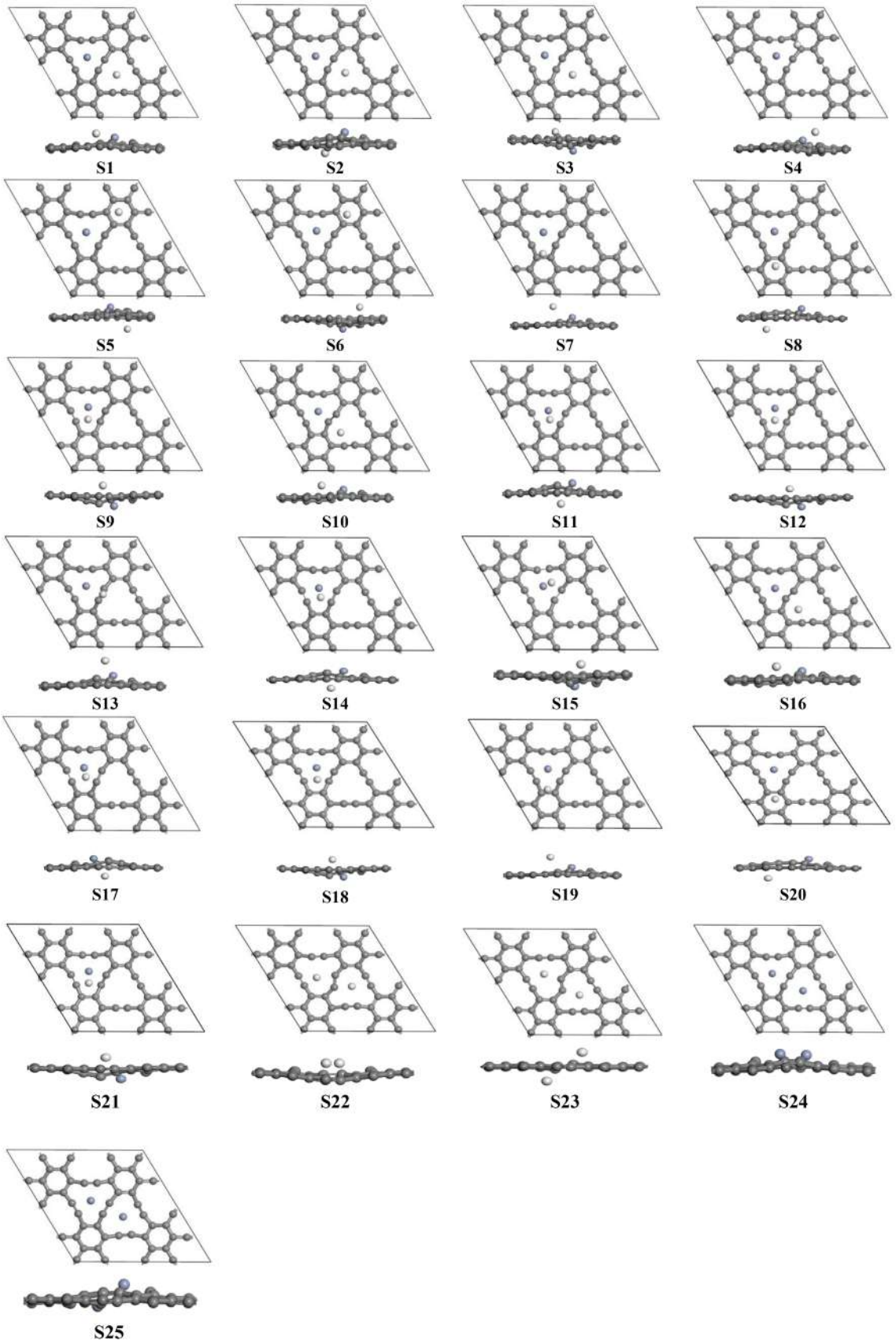

Fig. 3. Optimized structures of SCGY from top and side views.

Table 2
Initial adsorption sites of Sc and Cr atoms, Side of TMs, Average distance between Sc–GY (d1) and Cr–GY (d2), Adsorption energy (E_{ads}), and Hirshfeld charge of Sc (Q1) and Cr (Q2) in SCGY structures.

Structures	Initial Sc site	Initial Cr site	Side of TMs[a]	d1 (Å)	d2 (Å)	E_{ads}[b] (eV)	Q1 (*e*)	Q2 (*e*)
S1	H1	H1	U-U	1.171	0.772	−5.100	0.594	0.371
S2	H1	H1	D-U	1.474	0.671	−5.352	0.585	0.393
S3	H1	H1	U-D	1.562	0.458	−5.352	0.584	0.393
S4	H2	H1	U-U	1.726	0.676	−4.835	0.559	0.309
S5	H2	H1	D-U	1.675	0.629	−4.444	0.722	0.414
S6	H2	H1	U-D	2.049	0.587	−4.210	0.721	0.410
S7	B1	H1	U-U	1.618	0.518	−4.926	0.555	0.269
S8	B1	H1	D-U	2.071	0.648	−4.437	0.722	0.415
S9	B1	H1	U-D	1.263	0.714	−5.361	0.590	0.355
S10	B2	H1	U-U	0.905	0.526	−5.191	0.600	0.360
S11	B2	H1	D-U	1.528	0.620	−5.354	0.589	0.356
S12	B2	H1	U-D	1.388	0.587	−5.355	0.590	0.356
S13	B3	H1	U-U	1.991	0.368	−4.635	0.577	0.281
S14	B3	H1	D-U	1.882	0.265	−5.355	0.590	0.356
S15	B3	H1	U-D	1.721	0.443	−5.356	0.589	0.357
S16	T1	H1	U-U	0.851	0.489	−5.188	0.601	0.360
S17	T1	H1	D-U	1.543	0.613	−5.351	0.593	0.354
S18	T1	H1	U-D	1.523	0.633	−5.285	0.593	0.354
S19	T2	H1	U-U	1.754	0.651	−4.926	0.555	0.269
S20	T2	H1	D-U	1.747	0.524	−4.440	0.722	0.415
S21	T2	H1	U-D	1.278	0.698	−5.356	0.590	0.356
S22	H1-H1	–	U-U	1.041–1.043	–	−4.937	0.616–0.616	–
S23	H1-H1	–	U-D	1.587–1.586	–	−4.465	0.547–0.546	–
S24	–	H1-H1	U-U	–	1.035–1.036	−2.872	–	0.442–0.443
S25	–	H1-H1	U-D	–	0.687–0.686	−2.772	–	0.402–0.396

[a] Up (U) and Down (D) sides of the SCGY sheet.
[b] Adsorption energy of second metal (Sc) to Cr-decorated GY.

sheet. Unlike **S24**, the spin-up and spin-down states of the **S9** and **S22** structures are similar, exactly and their PDOS images are symmetric. While, for **S24** contributions of spin-up states are different from spin-down states. So, it can say that **S24** has magnetic property, but **S9** and **S22** don't show magnetic properties.

3.3. Capture of the single CO_2 molecule onto PGY and Sc or Cr-decorated GY

Our previous results for single CO_2 capture by intact GY and Sc or Cr-decorated GY reveal that for intact GY, H1 site and horizontal orientation is the best configuration with E_{ads} of −0.242 eV, and for Sc and Cr-decorated GY, top of TM and almost horizontal orientation are the best configurations with E_{ads} of −0.717 and −1.502 eV, respectively. Adsorption behavior of these systems was studied in details in our previous work [59]. Our results (adsorption energies) are similar to or even better than those of the recent theoretical studies about CO_2 adsorption on the Fe-doped penta-graphene (−0.157 eV), pristine phosphorene (−0.170 eV), P-doped graphene (−0.100 eV), C_2N monolayer (−0.200 eV) and TM atoms adsorbed on the single and double-vacancy graphene [14,70–73]. Fig. 6 shows the spin-polarized PDOS diagrams of the CO_2 adsorbed on pristine and Sc or Cr-decorated GY that were segmented to C_{sp}, C_{sp2}, CO_2, Sc and Cr atoms, as well total of the systems.

As shown in Fig. 6 (a), for the CO_2 adsorbed onto the PGY system, *p* orbitals of the C_{sp} and C_{sp2} atoms form the states close to the Fermi level. While, the contribution of *s* and *p* orbitals of CO_2 in the states near the Fermi level is almost zero. Also, there is a low overlap between CO_2 and GY orbitals in the bonding states region and under the Fermi level, which confirms a weak interaction between CO_2 and PGY. These images show that the system still is semiconductor even after CO_2 adsorption; however band gap has slightly changed (0.427 against 0.432 eV in

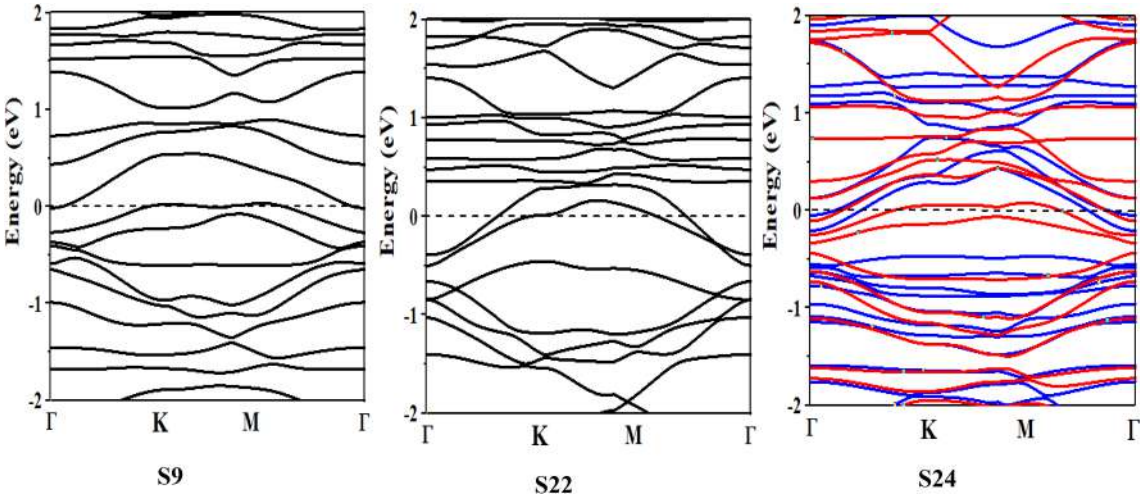

Fig. 4. Electronic band structure of: (a) **S9**, (b) **S22**, and (c) **S24** systems.

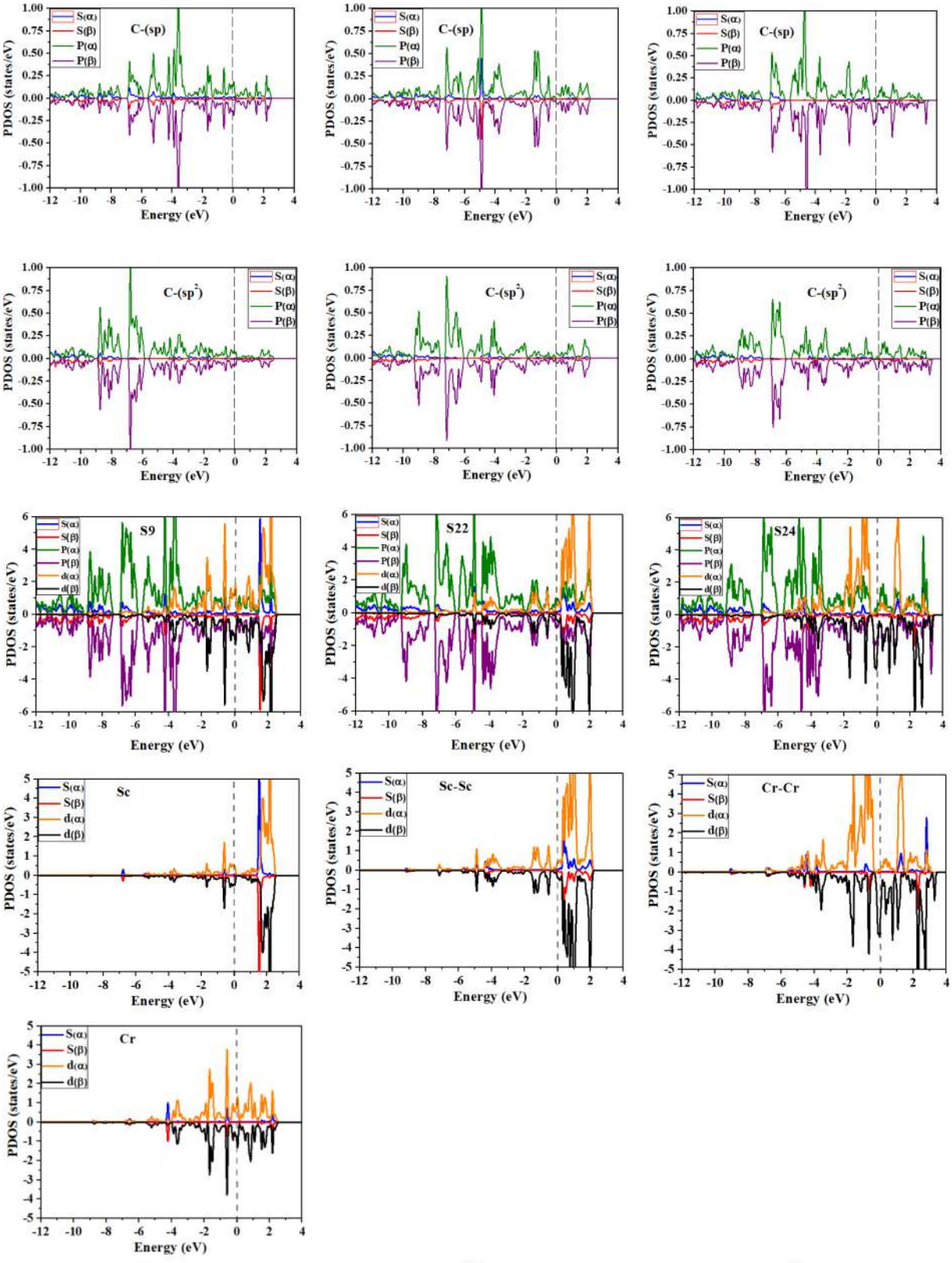

Fig. 5. PDOS images of: (a) **S9**, (b) **S22**, and (c) **S24** structures; each row is related to similar species.

absence of CO_2). Insertion of decorating Sc and Cr atoms causes substantial changes in PDOS images (Fig. 6 (b) and (c)). For instance, the peaks of CO_2 molecule show a shift to lower energy (negative shift). It is seen that in CO_2 adsorbed on Sc-GY, the bonding states are built by the C 2*p* orbitals of the GY and CO_2 molecule. Also, the *p* orbitals of the C_{sp}, $C_{sp2,}$ and Sc 3*d* orbitals form the states close to the Fermi level and CO_2 has no contribution in them. But, in CO_2 adsorbed on Cr-GY, not only the *p* orbitals of the C_{sp}, $C_{sp2,}$ and Cr 3*d* orbitals both also the *p* orbitals

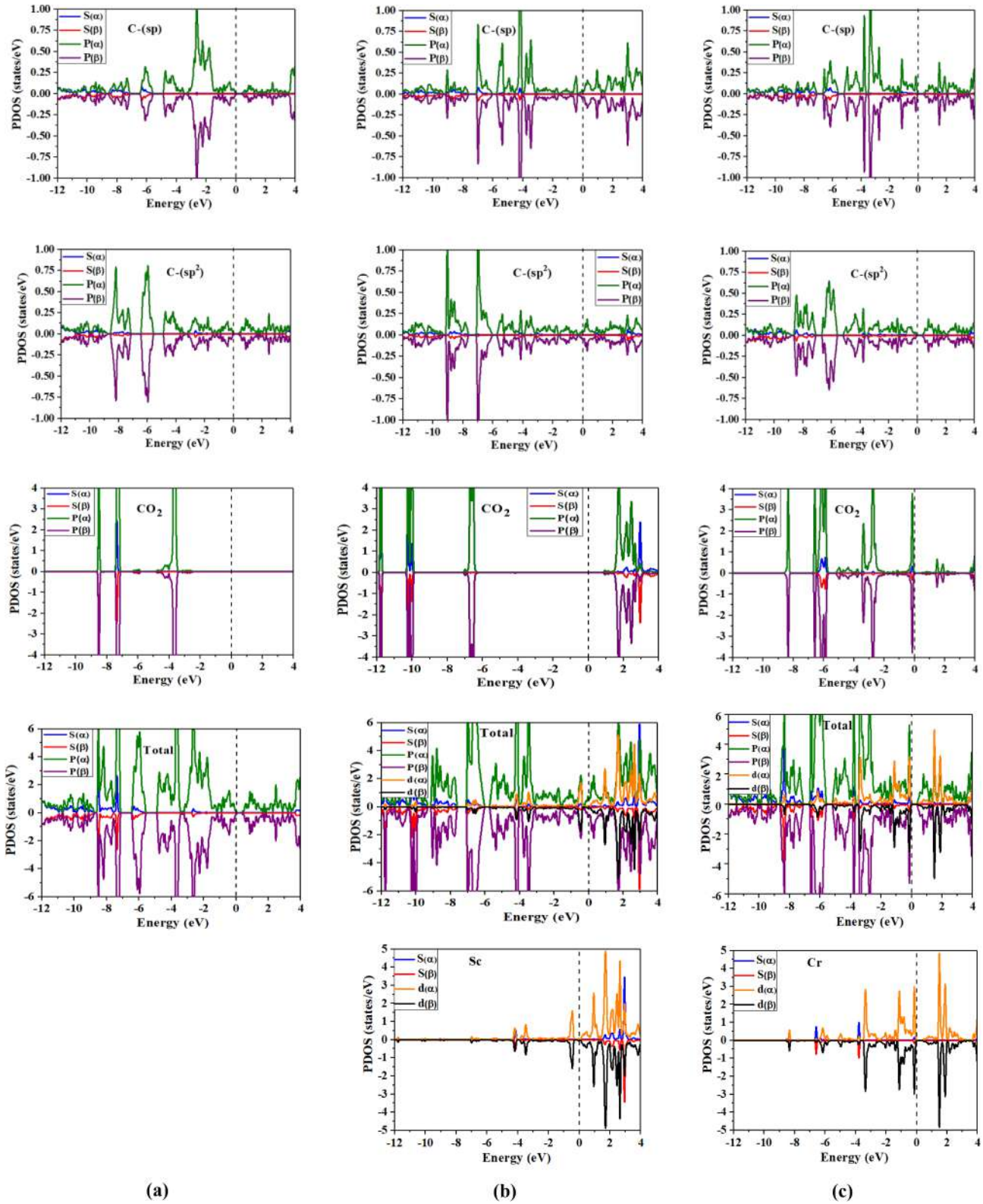

Fig. 6. PDOS images for adsorption of CO_2 onto: (a) pristine, (b) Sc-decorated, and (c) Cr-decorated GY systems.

of CO_2 participate in the states near the Fermi level. It seems that there are significant overlaps between the π states of the CO_2 and carbon atoms of GY, as well Cr 3*d* orbitals. But, for the CO_2-SC-GY system, these overlaps between states of CO_2 with states of the Sc-GY system are very lower. This topic confirms that E_{ads} of CO_2 on Cr-decorated GY is two times higher than it for Sc-decorated GY (-1.502 and -0.717 eV). In the next section, we will consider the synergetic effect of co-decorating with these two metals onto CO_2 adsorption behavior.

3.4. Capture of the single CO_2 molecule on SCGY

In the following, we studied the single CO_2 adsorption behavior on

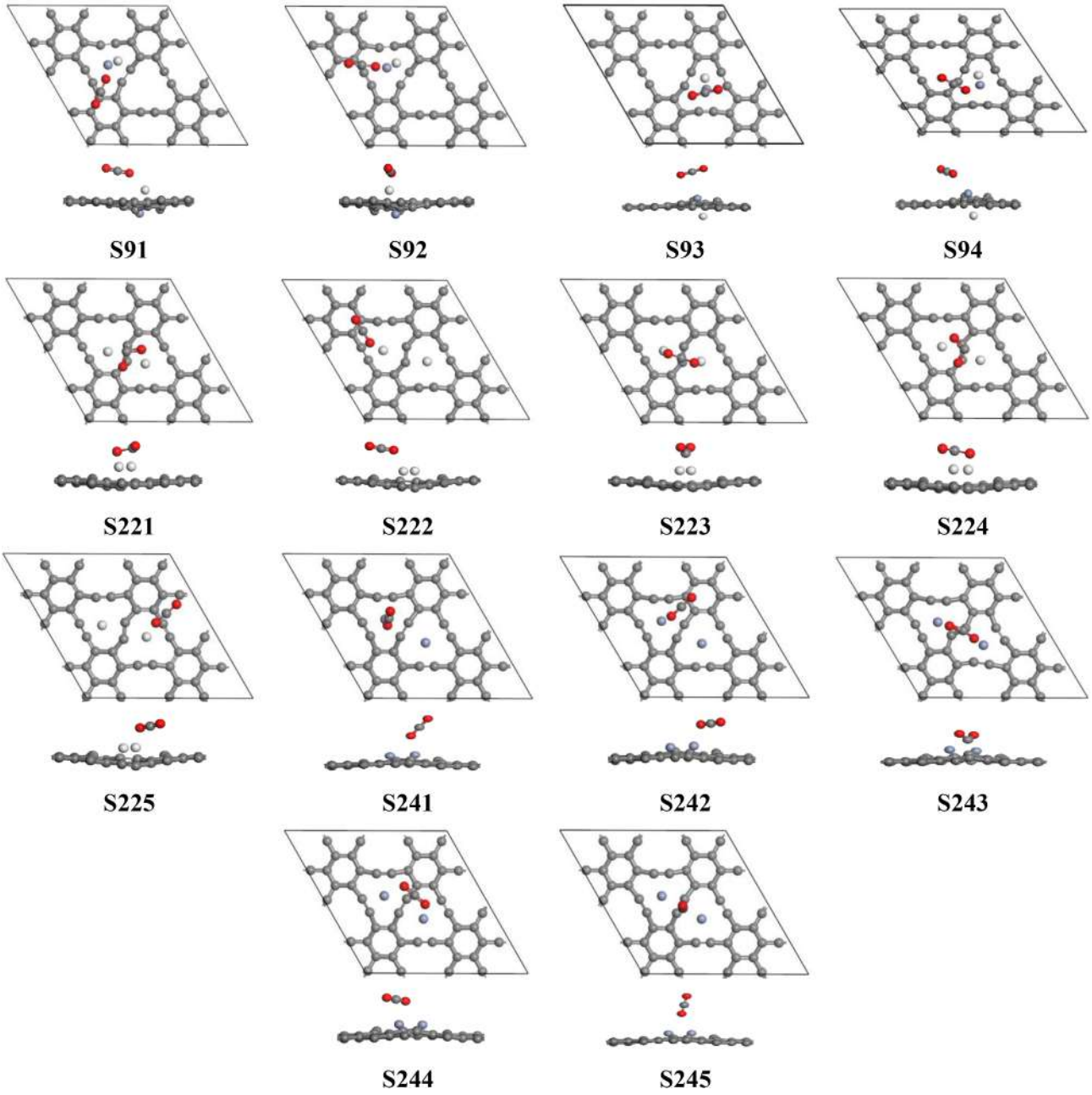

Fig. 7. The best optimized structures for adsorption of CO_2 onto SCGY from two views.

the SCGY structures. We put a single CO_2 molecule in vertical and horizontal directions on top of the Sc and Cr atoms in SCGY. Then, full geometry optimizations were done. The optimized structures with the best positions and orientations of the single CO_2 have been shown in Fig. 7. For this section, we consider **S9**, **S22** and **S24** for CO_2 capturing that were the best structures of SCGY and for nomination of them, we added an excess number after their names (Fig. 7).

Some of the structural properties of one CO_2 adsorbed on SCGY structures have been displayed in Table 3. Adsorption energy values in Table 3 show that among the sub-structures related to **S9** structure, **S91** is the most stable in which, the adsorption energy of CO_2 in adjacent of the Sc atom with horizontal direction is more favorable than when CO_2 adsorbed on the Sc-decorated GY, namely simultaneous presence of Sc and Cr atoms on GY improves E_{ads} of CO_2 on the Sc-decorated GY (E_{ads} about -0.795 compared to -0.717 eV). On the other hand, in **S93** and **S94** that CO_2 lies in adjacent to the Cr atom, E_{ads} decreases dramatically in comparison with when it lies onto Cr-decorated GY (-0.424 against -1.502 eV); namely, Sc has a decreasing effect on the E_{ads}. Also, among the sub-structures related to **S22**, **S223** is the most stable sub-structure. In **S223**, E_{ads} of CO_2 onto the Sc atoms is about 4 times more than E_{ads} of CO_2 onto Sc-decorated GY. These results indicate that simultaneous presence of two Sc atoms in the same side that CO_2 is horizontally along two metal atoms so that each O atom is almost top of an Sc atom (**S223** in Fig. 7) causes a synergetic effect happens and binds CO_2 to the carbon frame, strongly (-2.970 against -0.717 eV).

But in the **S243** sub-structure, concern to **S24,** that is the best of them, energetically, it is seen that E_{ads} of CO_2 onto the Cr atoms on the same side hasn't considerable increasing compared to when it is captured by Cr-decorated GY. These results indicate that the simultaneous presence of two Cr atoms in **S243** cannot create a synergetic effect to promote E_{ads} of CO_2 to GY framework. Generally and based on the results in Table 3, the CO_2 adsorption energies on **S91**, **S223**, and **S243** sub-structures are very better than recent theoretical study about CO_2 capture on N, S dual-doped graphene [11].

Table 3
The capture of one CO_2 on the **S9**, **S22** and **S24** structures; distance between CO_2 and GY (d1), CO_2 and decorating atoms (d2) (in Å), E_{ads} and band gap (E_g) (in eV), average C-O bond length of CO2 (l), C-O-C angle and Hirshfeld charge of Sc (Q1), Cr (Q2) and CO_2 (Q3) (in *e*).

Structure	CO_2 site	I.O.	F.O.	d1	d2	l	Angle	E_{ads}	Q1	Q2	Q3
S91	Top 0f Sc	H	H	3.032	1.395	1.173	176.5	−0.795	0.478	0.352	0.194
S92		V	H	3.056	1.452	1.173	176.4	−0.794	0.478	0.351	0.195
S93	Top 0f Cr	H	H	3.095	2.793	1.175	179.7	−0.203	0.589	0.327	0.021
S94		V	H	2.859	2.011	1.174	179.1	−0.424	0.583	0.345	0.112
S221	Top 0f Sc	H	Angular	2.427	1.182	1.325	113.2	−2.258	0.471 & 0.474	–	−0.454
S222		V	H	2.918	1.952	1.175	176.0	−0.774	0.451 & 0.551	–	0.204
S223	Bet 1[a]	H	Angular	2.612	1.558	1.278	130.4	−2.970	0.448 & 0.450	–	−0.373
S224	Bet 2[b]	H	Angular	2.549	1.196	1.317	114.2	−2.305	0.458 & 0.482	–	−0.434
S225	Bet 3[c]	V	H	2.709	1.878	1.174	176.7	−0.785	0.447 & 0.554	–	0.195
S241	Cr	H	Oblique	2.612	2.121	1.174	179.8	−0.248	–	0.381 & 0.381	0.152
S242		V	H	2.802	2.056	1.175	178.5	−0.410	–	0.381 & 0.382	0.138
S243	Bet 1	H	H	2.733	2.115	1.195	139.0	−1.754	–	0.382 & 0.374	0.138
S244	Bet 2	H	H	2.884	2.314	1.174	179.0	−0.352	–	0.389 & 0.385	0.073
S245	Bet 3	V	V	3.211	2.891	1.174	179.8	−0.182	–	0.398 & 0.391	0.045

[a] The single CO_2 between two decorating atoms with horizontal orientation along them.
[b] The single CO_2 between two decorating atoms with horizontal orientation across them.
[c] The single CO_2 between two decorating atoms with vertical orientation.

Fig. 8 shows the spin-polarized PDOS diagrams of the CO_2 adsorbed on **S91**, **S223**, and **S243** sub-structures that were segmented to C_{sp}, C_{sp2}, CO_2, Sc and Cr atoms, as well total DOS of system. As shown in Fig. 8 (a), the bonding states have been composed of C 2*p* orbitals of GY and CO_2, and Sc and Cr 3*d* orbitals, but the contribution of Cr atom is more than Sc atom. Also, the states near the Fermi level were composed of *p* orbitals of C_{sp}, $C_{sp2,}$ and 3*d* orbitals of Sc and Cr atoms in **S91**, but the CO_2 has no contribution in the states near the Fermi level. Furthermore, for Sc and Cr atoms, PDOS images reveal that Sc and Cr 3*d* and 4*s* orbitals donate part of their electrons to the empty π* bands of the carbon atoms of GY and some of these electrons back-donate to 3*d* orbitals. But, this back-donation in Cr atom is more than Sc atom (or Sc 4*s* orbitals donate less electron than Cr 4*s* orbitals to the empty C π* bands of GY; this is consistent with electron configuration of Cr: [Ar] $3d^5$ $4s^1$). More contribution of 3*d* states of Cr atom in bonding states in three sections of Fig. 8 confirms this conclusion. Also, this topic is in agreement with more positive charge of Sc than Cr in Table 3.

Because of less electron donation of Cr, in **S91** that Cr is on the opposite side of Sc, its influence on the E_{ads} of CO_2 is slight (−0.795 eV). So, it can be concluded that CO_2 adsorption energy onto **S91** is approximately equal to the Sc-decorated GY structure (−0.717 eV). While, for **S223** that there are two Sc atoms on the same side, E_{ads} of CO_2 is the most among all of them (−2.970 eV). Also, in **S243** that there are two Cr atoms, because they are on the same side, adsorption energy is partly high (−1.754 eV) and more than **S91**. It seems that there are many determining factors for E_{ads} such as electron donation of a metal atom, position, and side of a metal atom, as well spatial orientation and site of the CO_2 molecule.

There is another attractive point in Table 3. In the structures that electron transfers to CO_2 molecule and its charge is negative such as **S221**, **S223** and **S224**, E_{ads} are more than other structures, dramatically, (−2.258, −2.970 and −2.305 eV, respectively) that all of them are related to co-decoration with two Sc atoms. While, previous work obviously shows that in single Sc and Cr decorated GY, E_{ads} of CO_2 is almost twice for Cr compared to Sc atom (−1.502 against −0.717 eV) [59]. This confirms that the synergetic effect of two Sc atoms is more than two Cr atoms or even one Sc and one Cr atom. In these three structures, the angle of adsorbed CO_2 changes dramatically and from linear molecule coverts to an angular one.

As shown in Fig. 8 (b) and (c), the states near the Fermi level have been composed of the *p* orbitals of the C_{sp}, and C_{sp2} and 3*d* orbitals of Sc and Cr atoms in **S223** and **S243**, respectively. But, CO_2 molecule in the **S223** structure has a larger contribution near the Fermi level than **S91** and **S243**. In **S223**, CO_2 adsorption energy onto the Sc atoms is approximately 4 and 1.5 times of the CO_2 adsorption energies onto **S91** and **S243**, respectively. These results show that simultaneous presence of two Sc atoms in **S223** compared to Sc and Cr atoms in **S91** and two Cr atoms in **S243** has a more synergetic effect on the adsorption energy of CO_2 (−2.970 eV against −0.795 and −1.754 eV, respectively).

Fig. 9 displays the difference in electron density distribution images of **S91**, **S223** and **S243** structures to confirm the above results about the CO_2 adsorption. As shown in Fig. 9, especially (b) and (c) sections, there is significant charge transfer between the GY surface, CO_2 molecule, Sc and Cr atoms that is consistent with their strong interactions. For this reason, the mechanism of the CO_2 adsorption in the presence of two Sc or two Cr atoms in **S223** and **S243** structures is much stronger than the **S91** structure. This evidence is along with the results of the Hirshfeld charge analysis in Table 3. Also, these strong charge transfers and high adsorption energies cause considerable deformation in CO_2 structure adsorbed on the **S223** structure, namely C–O bond length in **S223** further increases than **S91** and **S243** (1.278 against 1.173 and 1.195 Å, respectively). Also, the O–C–O angle in **S223** is further decreases than **S91** and **S243** (130.4° against 176.5° and 139.0°, respectively).

In Fig. 10 overall comparison among the best structures for adsorption of CO_2 from the various category of intact and modified GY has been shown. It is seen that decoration with Sc and Cr atoms is a good approach to improve E_{ads} of CO_2, generally. But depending on the type and number of decorating atom(s), this promotion is different. Decoration of GY by one Sc or Cr atom improves E_{ads} of CO_2 about 3 and 6.2 times compared to intact GY. But simultaneous decoration with Sc and Cr atoms hasn't much effect on it. Surprisingly, however decoration with a Cr atom is more effective than an Sc atom (~2 times), but co-decoration with two Cr atoms only promotes E_{ads} ~ 1.2 times compared to single Cr-decorated GY, while this growth for using two Sc atoms compared to single Sc atom decoration is ~4.1 times.

3.5. Capture capacity of CO_2 onto PGY and *S223* structures

An important feature in identifying CCS of materials is the maximum CO_2 capture capacity of them [73]. So, to obtain the maximum number of CO_2 molecules adsorbed on the PGY and **S223** structures, we added CO_2 molecules step by step onto these structures and optimized them. We use $\bar{E}_{ads}$ and E_s to monitor CCS of these systems. Some of the obtained results have been reported in Table 4. We continued CO_2 addition up to reach the adsorption energy of step (E_s) to less than 0.1 eV as a criterion. For comparison, first, we added CO_2 molecule onto PGY. It is seen that PGY can only store three CO_2 molecules with E_{ads} of −0.249 eV/CO_2 that is about 18.63 wt% of CO_2 capture capacity (Table 4). Furthermore, the **S223** structure can hold 19 CO_2 molecules

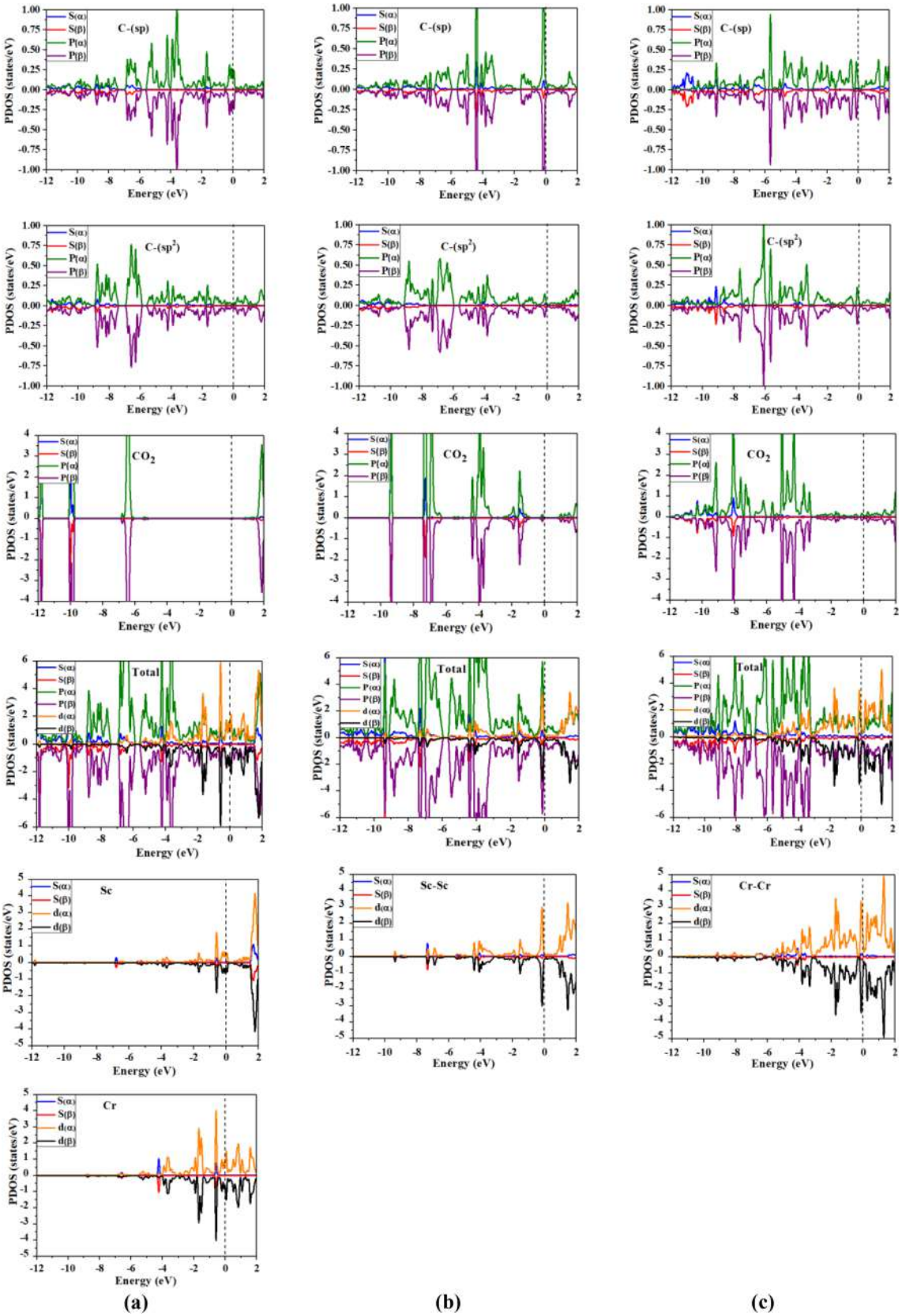

Fig. 8. PDOS images of the CO_2 adsorbed onto: (a) **S91**, (b) **S223**, and (c) **S243** structures.

with an average adsorption energy of -0.163 eV/CO_2 that is about 55.66 wt% for CO_2 capture capacity. These results show that the simultaneous presence of two Sc atoms in **S223** can promote CCS in GY structure, extremely. For PGY and **S223** with maximum CO_2 capture capacity, the optimized structures have been displayed in Fig. 11. However, the simultaneous presence of two Cr atoms or one Cr and one

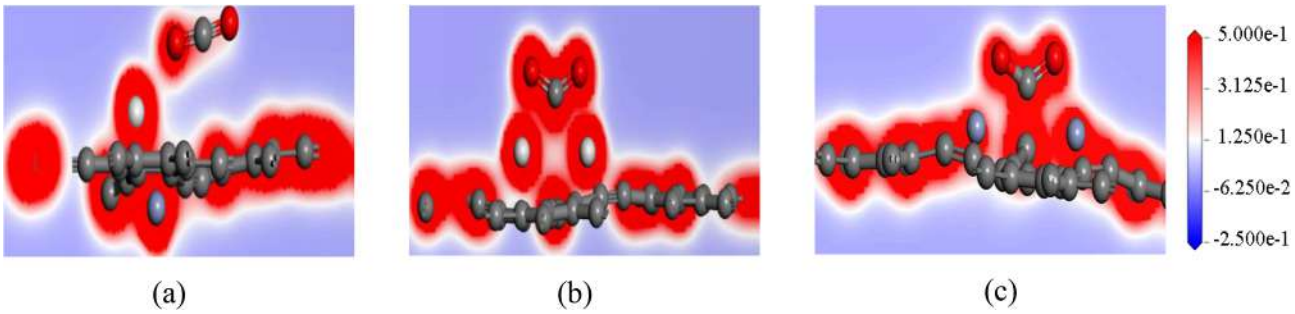

Fig. 9. The difference electron density images of (a) **S91**, (b) **S223,** and (c) **S243** structures; blue and red colors represent depletion and accumulation of charges, respectively. (For interpretation of the references to colour in this figure legend, the reader is referred to the web version of this article.)

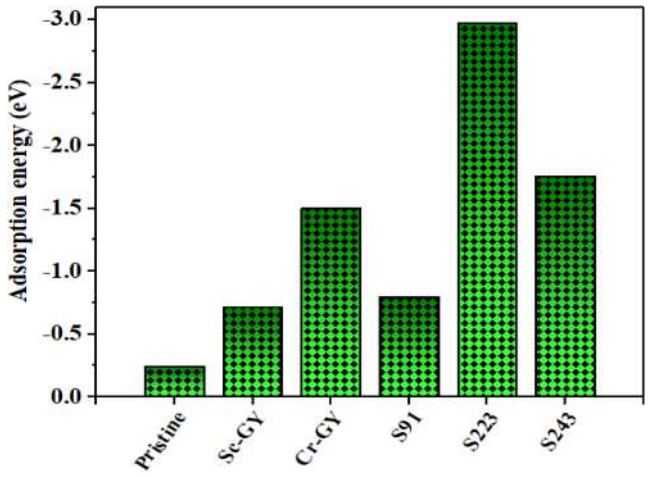

Fig. 10. Comparison of the best structures for CO_2 capturing competition.

Sc atom can also promote the CO_2 capture capacity of GY, but their influence isn't so much.

4. Conclusions

To evaluate co-decoration of GY by Sc and Cr atoms, we examined Sc atom in various sites of Cr-decorated GY, in which Cr was put in the H1 site. Also, co-decoration of GY by two Sc atoms or two Cr atoms was evaluated. The results show that H1 site is more favorable than other sites for Cr atom, but Sc atom lies in H3 site and the opposite side of Cr. When, Sc and Cr lie in two adjacent 12-membered rings, H1 sites and opposite sides are more favorable than others for them. Generally, from the viewpoint of energy, using Sc and Cr atoms as decorating metals is better than using from two Sc or Cr atoms. Therefore, it can say that configurations with Sc and Cr atoms in H3 and H1 sites and opposite sides are the most stable configurations and among these configurations, **S9** with E_{ads} of the second metal (Sc) about −5.361 eV is the most configuration, while, E_{ads} of Sc on GY is −4.856 eV. It seems that Sc and Cr have a synergetic effect of −0.505 eV (!) on this E_{ads}. From the viewpoint of E_{ads}, there is a difference between co-decorated GY systems with two similar (**S22** to **S25**) or different metal decorating atoms (**S1** to **S21**). For the first systems, up-up configurations are more stable than up-down ones, while for the latter it is contrariwise. Among three types of co-decorated GY, namely Sc-Cr, Sc-Sc, and Cr-Cr systems, only for the third one (such as **S24**) spin-up and spin-down states are different and spin polarization is observed and it shows a magnetic property. Also, the most adsorption energies of second metal for Sc-Sc and Cr-Cr co-decorated GY systems are related to **S22** and **S24** structures (about −4.937 and −2.872 eV, respectively) that are more than when these metals are added to PGY.

Evaluation of the adsorption behavior of CO_2 onto SCGY demonstrates that the highest E_{ads} of CO_2 is related to **S223** structure in which it is about ~4 times compared to single Sc-decorated GY (−2.970 against −0.717 eV). Calculations revealed that **S223** can capture and store up to 19 CO_2 molecules that are equal to 55.66 wt% of the system. In brief, E_{das} of CO_2 for PGY, Sc-GY, Cr-GY, Sc-Cr-GY, Sc-Sc-GY, and Cr-Cr-GY are about −0.242, −0.717, −1.502, −0.795, −2.970 and −1.754 eV, respectively. These findings show that co-decoration of GY and graphdiyne with various metals can be used as not only the subject of research works but also the promising candidate for the CO_2 capture, detection, and removal applications in the future.

Declaration of Competing Interest

The authors declare that they have no known competing financial interests or personal relationships that could have appeared to influence the work reported in this paper.

Table 4
$\bar{E}_{ads}$ and E_s (in eV), and maximum CO_2 capture capacity (wt. %) in PGY and **S223** structures.

Structure	No. of CO_2	$\bar{E}_{ads}$	E_s	Wt.%	Structure	No. of CO_2	$\bar{E}_{ads}$	E_s	Wt.%
PGY	1	−0.242	−0.242		**S223**	9	−0.777	−0.448	
	2	−0.193	−0.174			10	−0.702	−0.298	
	3	−0.249	−0.343	18.63		11	−0.669	−0.330	
	4	−0.206	−0.089			12	−0.635	−0.265	
S223	1	−2.970	−2.970			13	−0.612	−0.336	
	2	−1.835	−0.700			14	−0.579	−0.151	
	3	−1.342	−0.356			15	−0.560	−0.298	
	4	−1.096	−0.358			16	−0.557	−0.508	
	5	−0.918	−0.205			17	−0.542	−0.302	
	6	−0.971	−1.236			18	−0.528	−0.188	
	7	−0.881	−0.342			19	−0.516	−0.163	55.66
	8	−0.819	−0.382			20	−0.504	−0.027	

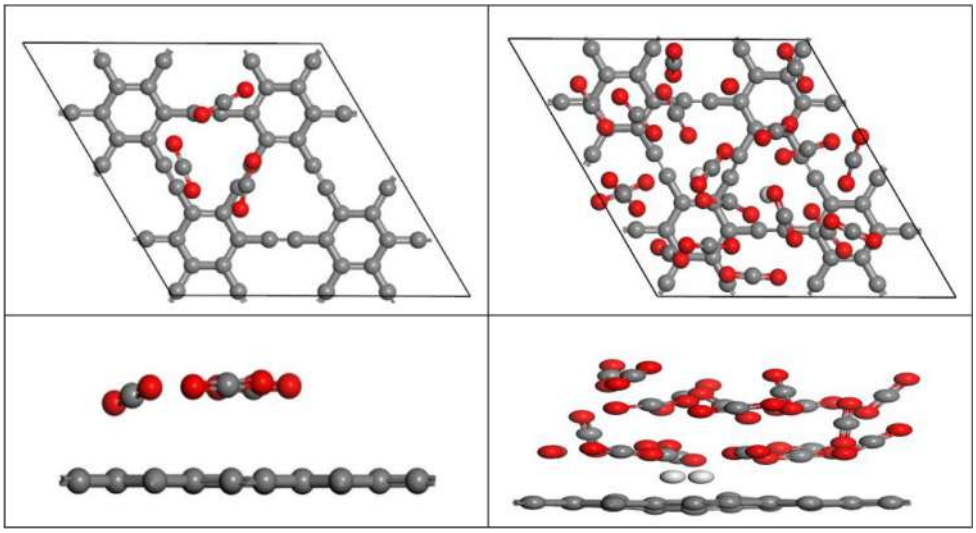

Fig. 11. Maximum number of CO_2 capture onto: PGY (3 CO_2) (left), and **S223** structures (19 CO_2) (right) from the top and side views.

Acknowledgment

This work was supported by the University of Kashan (Grant No. 785097/4), authors are grateful for this support.

References

[1] D. McCollum, N. Bauer, K. Calvin, A. Kitous, K. Riahi, Fossil resource and energy security dynamics in conventional and carbon-constrained worlds, Clim. Change 123 (2014) 413–426.
[2] S.J. Davis, K. Caldeira, H.D. Matthews, Future CO_2 emissions and climate change from existing energy infrastructure, Science 329 (2010) 1330–1333.
[3] R.S. Haszeldine, Carbon capture and storage: how green can black be? Science 325 (2009) 1647–1652.
[4] D.W. Keith, Why capture CO_2 from the atmosphere? Science 325 (2009) 1654–1655.
[5] S. Chu, A. Majumdar, Opportunities and challenges for a sustainable energy future, Nature 488 (2012) 294–303.
[6] H. Choi, Y.C. Park, Y.-H. Kim, Y.S. Lee, Ambient carbon dioxide capture by boron-rich boron nitride nanotube, J. Am. Chem. Soc. 133 (2011) 2084–2087.
[7] X. Tan, L. Kou, S.C. Smith, Layered graphene–hexagonal BN nanocomposites: experimentally feasible approach to charge-induced switchable CO_2 capture, ChemSusChem 8 (2015) 2987–2993.
[8] X. Tan, L. Kou, H.A. Tahini, S.C. Smith, Conductive graphitic carbon nitride as an ideal material for electrocatalytically switchable CO_2 capture, Sci. Rep. 5 (2015) 17636.
[9] T. Hussain, H. Vovusha, T. Kaewmaraya, A. Karton, V. Amornkitbamrung, R. Ahuja, Graphitic carbon nitride nano sheets functionalized with selected transition metal dopants: an efficient way to store CO_2, Nanotechnology 29 (2018) 415502.
[10] Y. Jiao, A. Du, Z. Zhu, V. Rudolph, S.C. Smith, A density functional theory study of CO_2 and N_2 adsorption on aluminium nitride single walled nanotubes, J. Mater. Chem. 20 (2010) 10426–10430.
[11] J. Li, M. Hou, Y. Chen, W. Cen, Y. Chu, S. Yin, Enhanced CO_2 capture on graphene via N, S dual-doping, Appl. Surface Sci. 399 (2017) 420–425.
[12] X. Li, Y. Cheng, H. Zhang, S. Wang, Z. Jiang, R. Guo, H. Wu, Efficient CO_2 capture by functionalized graphene oxide nanosheets as fillers to fabricate multi-permselective mixed matrix membranes, ACS Appl. Mater. Interfaces 7 (2015) 5528–5537.
[13] X. Tan, H.A. Tahini, S.C. Smith, Borophene as a promising material for charge-modulated switchable CO_2 capture, ACS Appl. Mater. Interfaces 9 (2017) 19825–19830.
[14] H.-P. Zhang, A. Du, Q.-B. Shi, Y. Zhou, Y. Zhang, Y. Tang, Adsorption behavior of CO_2 on pristine and doped phosphorenes: a dispersion corrected DFT study, J. CO_2 Utilization 24 (2018) 463–470.
[15] J. Wang, Q. Liu, An efficient one-step condensation and activation strategy to synthesize porous carbons with optimal micropore sizes for highly selective CO_2 adsorption, Nanoscale 6 (2014) 4148–4156.
[16] Z. Jia, Y. Li, Z. Zuo, H. Liu, C. Huang, Y. Li, Synthesis and properties of 2D carbon-graphdiyne, Acc. Chem. Res. 50 (2017) 2470–2478.
[17] R.H. Baughman, H. Eckhardt, M. Kertesz, Structure-property predictions for new planar forms of carbon: layered phases containing sp^2 and sp atoms, J. Chem. Phys. 87 (1987) 6687.
[18] Y. Li, L. Xu, H. Liu, Y. Li, Graphdiyne and graphyne: from theoretical predictions to practical construction, Chem. Soc. Rev. 43 (2014) 2572–2586.
[19] C. Huang, Y. Li, N. Wang, Y. Xue, Z. Zuo, H. Liu, Y. Li, Progress in research into 2D graphdiyne-based materials, Chem. Rev. 118 (2018) 7744–7803.
[20] H. Tang, C.M. Hessel, J. Wang, N. Yang, R. Yu, H. Zhao, D. Wang, Two-dimensional carbon leading to new photoconversion processes, Chem. Soc. Rev. 43 (2014) 4281–4299.
[21] D. Malko, C. Neiss, F. Vines, A. Görling, Competition for graphene: graphynes with direction-dependent dirac cones, Phys. Rev. Lett. 108 (2012) 086804.
[22] H. Huang, W. Duan, Z. Liu, The existence/absence of Dirac cones in graphynes, New J. Phys. 15 (2013) 023004.
[23] P. Jiang, H. Liu, L. Cheng, D. Fan, J. Zhang, J. Wei, J. Liang, J. Shi, Thermoelectric properties of γ-graphyne from first-principles calculations, Carbon 113 (2017) 108–113.
[24] X. Hou, Z. Xie, C. Li, G. Li, Z. Chen, Study of electronic structure, thermal conductivity, elastic and optical properties of α, β, γ-graphyne, Materials 11 (2018) 188.
[25] Z.-G. Shao, Z.-L. Sun, Optical properties of α-, β-, γ-, and 6,6,12-graphyne structures: first-principle calculations, Physica E 74 (2015) 438–442.
[26] J. Kang, J. Li, F. Wu, S.-S. Li, J.-B. Xia, Elastic, electronic, and optical properties of two-dimensional graphyne sheet, J. Phys. Chem. C 115 (2011) 20466–20470.
[27] B. Bhattacharya, U. Sarkar, The effect of boron and nitrogen doping in electronic, magnetic, and optical properties of graphyne, J. Phys. Chem. C 120 (2016) 26793–26806.
[28] J. Sarma, R. Chowdhury, R. Jayaganthan, Graphyne-based single electron transistor: ab initio analysis, Nano 9 (2014) 1450032.
[29] M. Shams, A. Reisi-Vanani, Potassium decorated γ-graphyne as hydrogen storage medium: Structural and electronic properties, Int. J. Hydrogen Energy 44 (2019) 4907–4918.
[30] S. Kumar, T.J. Dhilip Kumar, Electronic structure calculations of hydrogen storage in lithium-decorated metal–graphyne framework, ACS Appl. Mater. Interfaces 9 (2017) 28659–28666.
[31] F. Akbari, A. Reisi-Vanani, M.H. Darvishnejad, DFT study of the electronic and structural properties of single Al and N atoms and Al-N co-doped graphyne toward hydrogen storage, Appl. Surf. Sci. 488 (2019) 600–610.
[32] J. Li, S. Li, Q. Liu, C. Yin, L. Tong, C. Chen, J. Zhang, Synthesis of hydrogen-substituted graphyne film for lithium–sulfur battery applications, Small 15 (2019) 1805344.
[33] C. Yang, Y. Li, Y. Chen, Q. Li, L. Wu, X. Cui, Mechanochemical synthesis of γ-graphyne with enhanced lithium storage performance, Small 15 (2019) 1804710.
[34] P. Sang, L. Zhao, J. Xu, Z. Shi, S. Guo, Y. Yu, H. Zhu, Z. Yan, W. Guo, Excellent membranes for hydrogen purification: Dumbbell-shaped porous γ-graphynes, Int. J. Hydrogen Energy 42 (2017) 5168–5176.
[35] P. Zhang, Q. Song, J. Zhuang, X.-J. Ning, First-principles study of gas adsorption on γ-graphyne, Chem. Phys. Lett. 689 (2017) 185–189.
[36] V. Nagarajan, S. Dharani, R. Chandiramouli, Density functional studies on the binding of methanol and ethanol molecules to graphyne nanosheet, Comput. Theor. Chem. 1125 (2018) 86–94.
[37] P. Wu, P. Du, H. Zhang, C. Cai, Graphyne-supported single Fe atom catalysts for CO oxidation, PCCP 17 (2015) 1441–1449.
[38] D. Ma, T. Li, Q. Wang, G. Yang, C. He, B. Ma, Z. Lu, Graphyne as a promising substrate for the noble-metal single-atom catalysts, Carbon 95 (2015) 756–765.
[39] K. Srinivasu, S.K. Ghosh, Transition metal decorated graphyne: an efficient catalyst for oxygen reduction reaction, J. Phys. Chem. C 117 (2013) 26021–26028.
[40] H.J. Kwon, Y. Kwon, T. Kim, Y. Jung, S. Lee, M. Cho, S. Kwon, Enhanced competitive adsorption of CO_2 and H_2 on graphyne: a density functional theory study, AIP Adv. 7 (2017) 125013.
[41] Y. Guo, Z. Chen, W. Wu, Y. Liu, Z. Zhou, Adsorption of NO_x (x = 1, 2) gas molecule on pristine and B atom embedded γ-graphyne based on first-principles study, Appl. Surf. Sci. 455 (2018) 484–491.
[42] F. Mofidi, A. Reisi-Vanani, Sensing and elimination of the hazardous materials such

as Sarin by metal functionalized γ-graphyne surface: A DFT study, J. Mol. Liq. 286 (2019) 110929.
[43] X. Kong, Y. Huang, Q. Liu, Two-dimensional boron-doped graphyne nanosheet: a new metal-free catalyst for oxygen evolution reaction, Carbon 123 (2017) 558–564.
[44] T. He, S.K. Matta, A. Du, Single tungsten atom supported on N-doped graphyne as a high-performance electrocatalyst for nitrogen fixation under ambient conditions, Phys. Chem. Chem. Phys. 21 (2019) 1546–1551.
[45] M.H. Darvishnejad, A. Reisi-Vanani, Multiple CO_2 capture in pristine and Sr-decorated graphyne: A DFT-D3 and AIMD study, Comput. Mater. Sci. 176 (2020) 109539.
[46] M.A. Fulazzaky, Study of the dispersion and specific interactions affected by chemical functions of the granular activated carbons, Environ. Nanotechnol. Monit. Manage. 12 (2019) 100230.
[47] S. Kim, A.R. Puigdollers, P. Gamallo, F. Viñes, J.Y. Lee, Functionalization of γ-graphyne by transition metal adatoms, Carbon 120 (2017) 63–70.
[48] X. Li, D.-H. Xing, Systematic theoretical study of electronic structures and stability of transition-metal adsorbed graphdiyne clusters, J. Phys. Chem. C 123 (2019) 8843–8850.
[49] L. Zhang, H. Wu, Metal decorated graphyne and its boron nitride analog as versatile materials for energy storage: Providing reference for the Lithium-ion battery of wireless sensor nodes, Int. J. Hydrogen Energy 41 (2016) 17471–17483.
[50] J. Ren, N.C. Zhang, S.B. Zhang, P.P. Liu, Effect of 3d-transition metal doping concentration on electronic structure and magnetic properties of Γ-graphyne, Fullerenes, Nanotubes, Carbon Nanostruct. 27 (2019) 684–694.
[51] Z. Lu, P. Lv, D. Ma, X. Yang, S. Li, Z. Yang, Detection of gas molecules on single Mn adatom adsorbed graphyne: a DFT-D study, J. Phys. D Appl. Phys. 51 (2018) 065109.
[52] X. Chen, P. Gao, L. Guo, Y. Wen, D. Fang, B. Gong, Y. Zhang, S. Zhang, High-efficient physical adsorption and detection of formaldehyde using Sc-and Ti-decorated graphdiyne, Phys. Lett. A 381 (2017) 879–885.
[53] B. Delley, From molecules to solids with the $DMol^3$ approach, J. Chem. Phys. 113 (2000) 7756–7764.
[54] J.P. Perdew, K. Burke, M. Ernzerhof, Generalized gradient approximation made simple, Phys. Rev. Lett. 77 (1996) 3865.
[55] B. Delley, Hardness conserving semilocal pseudopotentials, Phys. Rev. B 66 (2002) 155125.
[56] S. Ehrlich, J. Moellmann, W. Reckien, T. Bredow, S. Grimme, System-dependent dispersion coefficients for the DFT-D3 treatment of adsorption processes on ionic surfaces, ChemPhysChem 12 (2011) 3414–3420.
[57] S. Grimme, J. Antony, S. Ehrlich, H. Krieg, A consistent and accurate ab initio parametrization of density functional dispersion correction (DFT-D) for the 94 elements H-Pu, J. Chem. Phys. 132 (2010) 154104.
[58] S. Grimme, Semiempirical GGA-type density functional constructed with a long-range dispersion correction, J. Comput. Chem. 27 (2006) 1787–1799.
[59] M.H. Darvishnejad, A. Reisi-Vanani, Density functional theory study of CO_2 capture and storage promotion using manipulation of graphyne by 3d and 4d transition metals, Int. J. Quantum Chem. (2020).
[60] J. He, S.Y. Ma, P. Zhou, C. Zhang, C. He, L. Sun, Magnetic properties of single transition-metal atom absorbed graphdiyne and graphyne sheet from DFT + U calculations, J. Phys. Chem. C 116 (2012) 26313–26321.
[61] X. Gao, Y. Zhou, Y. Tan, S. Liu, Z. Cheng, Z. Shen, Graphyne doped with transition-metal single atoms as effective bifunctional electrocatalysts for water splitting, Appl. Surf. Sci. 492 (2019) 8–15.
[62] B. Kang, J.Y. Lee, Graphynes as promising cathode material of fuel cell: improvement of oxygen reduction efficiency, J. Phys. Chem. C 118 (2014) 12035–12040.
[63] A. Mohajeri, A. Shahsavar, Light metal decoration on nitrogen/sulfur codoped graphyne: An efficient strategy for designing hydrogen storage media, Physica E 101 (2018) 167–173.
[64] Y. Wang, Y. Ji, M. Li, P. Yuan, Q. Sun, Y. Jia, Li and Ca Co-decorated carbon nitride nanostructures as high-capacity hydrogen storage media, J. Appl. Phys. 110 (2011) 094311.
[65] Y.-J. Wang, H. Fan, A. Ignaszak, L. Zhang, S. Shao, D.P. Wilkinson, J. Zhang, Compositing doped-carbon with metals, non-metals, metal oxides, metal nitrides and other materials to form bifunctional electrocatalysts to enhance metal-air battery oxygen reduction and evolution reactions, Chem. Eng. J. 348 (2018) 416–437.
[66] Y. Guo, P. Yuan, J. Zhang, Y. Hu, I.S. Amiinu, X. Wang, J. Zhou, H. Xia, Z. Song, Q. Xu, Carbon nanosheets containing discrete Co-N x-B y-C active sites for efficient oxygen electrocatalysis and rechargeable Zn–air batteries, ACS Nano 12 (2018) 1894–1901.
[67] J.M. Walker, S.A. Akbar, P.A. Morris, Synergistic effects in gas sensing semiconducting oxide nano-heterostructures: a review, Sens. Actuators, B 286 (2019) 624–640.
[68] P. Liu, Y. Hu, X. Liu, T. Wang, P. Xi, S. Xi, D. Gao, J. Wang, Cu and Co nanoparticle-Co-decorated N-doped graphene nanosheets: a high efficiency bifunctional electrocatalyst for rechargeable Zn–air batteries, J. Mater. Chem. A 7 (2019) 12851–12858.
[69] A. De, J. Datta, Synergistic combination of Pd and Co catalyst nanoparticles over self-designed MnO2 structure: green synthetic approach and unprecedented electrode kinetics in direct ethanol fuel cell, ACS Sustainable Chem. Eng. 6 (2018) 13706–13718.
[70] C.-P. Zhang, B. Li, Z.-G. Shao, First-principle investigation of CO and CO_2 adsorption on Fe-doped penta-graphene, Appl. Surf. Sci. 469 (2019) 641–646.
[71] M.D. Esrafili, Electric field assisted activation of CO_2 over P-doped graphene: A DFT study, J. Mol. Graph. Model. 90 (2019) 192–198.
[72] S.S. Deshpande, M.D. Deshpande, T. Hussain, R. Ahuja, Investigating CO_2 storage properties of C_2N monolayer functionalized with small metal clusters, J. CO_2 Utilization 35 (2020) 1–13.
[73] S.A. Tawfik, X. Cui, S. Ringer, C. Stampfl, Multiple CO_2 capture in stable metal-doped graphene: a theoretical trend study, RSC Adv. 5 (2015) 50975–50982.